The local structure of the azobenzene/aniline reaction intermediate on TiO_2(110)

D. Kreikemeyer-Lorenzo[1] W. Unterberger[1], D.A. Duncan[2], T.J. Lerotholi[3], D.P. Woodruff[2*]

[1] *Fritz-Haber-Institut der Max-Planck-Gesellschaft, Faradayweg 4-6, 14195, Berlin, Germany*

[2] *Physics Department, University of Warwick, Coventry CV4 7AL, UK*

[3] *School of Chemistry, University of Witwatersrand, PO Wits, Johannesburg, 2050, South Africa*

Abstract

Scanned-energy mode photoelectron diffraction (PhD) and near-edge X-ray absorption fine structure (NEXAFS) have been used to study the surface species, previously proposed to be phenyl imide, C_6H_5N-, on rutile TiO_2(110) following exposure to either azobenzene or aniline. All measurements are consistent with the two reactants forming a common surface species in the same local adsorption site. N K-edge NEXAFS confirms the scission of the N=N bond in azobenzene, while C K-edge NEXAFS shows the phenyl ring to be intact with the molecular plane tilted relative to the surface normal and not aligned in either principle azimuth of the surface. N 1s PhD data indicate that the N atom bonds atop a surface five-fold-coordinated Ti atom, most probably at a Ti-N bondlength of 1.77±0.05 Å, and not bridging two such atoms, as had been suggested. This atop geometry is favoured by recent density functional theory (DFT) calculations, but more quantitative aspects of the DFT result are not in agreement with the conclusions of our experimental study.

Keywords: surface structure, TiO_2; azobenzene; aniline; photoelectron diffraction; molecular adsorption

[*] Corresponding author. Email d.p.woodruff@warwick.ac.uk

1. Introduction

The rutile-phase TiO_2(110) surface is the most-studied of all oxide surfaces (e.g. [1,2, 3]), in large part motivated by the known importance of titania in photocatalysis, gas sensors and as a support in a range of heterogeneous catalysts. Particular interest in recent years has centred on the properties of Au nanoparticles on titania following the discovery that this system is an effective catalysis for low-temperature oxidation of CO [4]. This combination has also been shown more recently to act as a high-yield catalyst in the synthesis of aromatic compounds [5, 6] including the synthesis of azobenzene ($C_6H_5N=NC_6H_5$) via oxidation of aniline ($C_6H_5NH_2$) (see Fig. 1). Somewhat intriguingly, it was found [6] that TiO_2 in the absence of the Au nanoparticles was also effective, and highly selective, in azobenzene synthesis. This led to a careful UHV surface science study of the interaction of azobenzene and aniline with both the rutile-phase TiO_2(110) and anatase-phase TiO_2(101) surfaces by Li, Diebold and coworkers [7, 8] who found evidence for a single surface reaction intermediate, produced by interaction with either azobenzene or aniline on both surfaces. On the rutile TiO_2(110) surface they found that adsorption of either molecule at full coverage leads to the formation of a c(2x2) ordered molecular phase, as seen both with low energy electron diffraction (LEED) and scanning tunnelling microscopy (STM). The STM images appear to be independent of the initial reactant molecule, as do the X-ray photoelectron spectroscopy (XPS) data from both the substrate and the molecular constituent atoms. The common molecular adsorbate species was thus assigned to phenyl imide (C_6H_5N-), produced either by N=N bond scission of azobenzene, or by dehydrogenation of aniline.

Here we present the results of further investigations of this system using the techniques of scanned-energy mode photoelectron diffraction (PhD) and near-edge X-ray absorption fine structure (NEXAFS). The PhD technique [9, 10] exploits the coherent interference of the directly emitted component of a photoelectron wavefield from an adsorbate atom with other components of the same wavefield elastically scattered by the surrounding atoms. Scanning the photon energy leads to changes in the photoelectron energy, and thus the

photoelectron wavelength, causing different scattering paths to switch in and out of phase with the directly-emitted wavefield. The resulting modulations in the measured intensity can be interpreted in terms of the different scattering paths associated with a particular adsorption geometry, through the use of multiple scattering simulations for different trial structures. In the present case, the use of N 1s PhD data allows us to determine the adsorption site of the expected bonding N atom on the TiO_2(110) surface and the associated Ti-N bondlength. We can also compare the local adsorption geometry of the molecular species formed by exposure to the two different reactant molecules, azobenzene and aniline. C K-edge NEXAFS provides information on the integrity of the aromatic ring in the adsorbed molecular species, and on its orientation. N K-edge NEXAFS allows us to establish independently whether the N=N bond scission occurs following exposure to azobenzene.

2. Experimental and computational details

The experiments were conducted in an ultra-high vacuum surface science chamber equipped with facilities for sample cleaning, heating and cooling. This instrument was installed on the UE56/2-PGM-2 beamline of BESSY II which comprises a 56 mm period undulator followed by a plane grating monochromator [11]. Sample characterisation *in situ* was achieved by low energy electron diffraction (LEED) and by soft-X-ray photoelectron spectroscopy (SXPS) using the incident synchrotron radiation. These wide-scan SXPS spectra, and the narrow-scan N 1s spectra used in the PhD measurements, were obtained using an Omicron EA-125HR 125 mm mean radius hemispherical electrostatic analyser, equipped with seven-channeltron parallel detection, which was mounted at a fixed angle of 60° to the incident X-radiation in the same horizontal plane as that of the polarisation vector of the radiation.

A clean well-characterised rutile TiO_2(110) surface was prepared by briefly bombarding with Ar^+ ions at an energy of 500 eV, followed by annealing in UHV at ~800 K for 10 minutes. The sample was then annealed at ~700 K in an oxygen atmosphere of $2x10^{-7}$ mbar for 10 minutes followed by a brief flash to ~1000 K. Oxygen dosing is known to

heal oxygen surface vacancies [1] that can arise from multiple re-cleaning cycles using ion bombardment and UHV annealing alone. This treatment led to a sharp (1x1) LEED pattern and a Ti 2p photoemission spectrum showing no detectable high kinetic energy shoulder, indicative of a low concentration of surface oxygen vacancies. The sample colour was dark blue, consistent with a concentration of bulk defects sufficient to render the sample conducting. Aniline and azobenzene (Sigma-Aldrich, 99.5% and 99% purity, respectively), subjected to freeze-thaw pumping cycles *in situ*, were dosed from the vapour phase at 300 K for all the preparations studied in UHV, although low temperature (150 K) dosing was also used to provide additional system characterisation. The azobenzene was heated to ~370 K to achieve a sufficiently high vapour pressure for the dosing, with the sample facing the gas inlet. Dosing of both species was checked using a mass spectrometer mounted on the chamber to monitored the gas phase components.

NEXAFS spectra from the dosed surfaces were measured in the Auger electron mode by setting the electron energy analyser to an energy in the range of the KLL Auger peak of the relevant element (C and N) and measuring the yield as a function of photon energy.

N 1s PhD data were obtained from the adsorbed species by recording a sequence of photoelectron energy distribution curves (EDCs) around this photoemission peak, at equal steps in photon energy, in the photoelectron kinetic energy range of ~ 60-320 eV. These data were measured at several different polar emission angles in the range 0° to 60°, and in the two principal azimuths, [001] and [$1\bar{1}0$] (see Fig. 2), although at polar angle greater than 30° no clear modulations above the noise level could be discerned. Data reduction followed our general PhD methodology (e.g. [9, 10]), in which each of the individual N 1s EDCs was fitted by the sum of a Gaussian peak, a step and a template background. The integrated peak areas were then plotted as a function of photoelectron energy, $I(E)$, and each final PhD modulation spectrum, $\chi(E)$, was obtained by subtraction of, and normalisation by, a smooth spline function, $I_0(E)$, representing the non-diffractive intensity and instrumental factors.

3. Results

3.1 SXPS and NEXAFS

Fig. 3 shows the SXP spectra in the energy ranges of the Ti 2p, O 1s, N 1s and C 1s emission peaks from the clean surface and following nominal saturation doses at room temperature of the two reactant molecules. The spectra recorded following aniline exposure are almost identical to those obtained following azobenzene exposure; the absence of chemical shifts in these pairs of spectra indicates that the same surface species is formed by the two molecules. In common with the results of Li and Diebold [7], however, we note a very small shift (~0.1 eV) of *all* peaks to lower kinetic energy (higher binding energy) after reaction with aniline. These authors suggest that this is due to band bending at the surface. While scission of the N=N bond in azobenzene would lead to *only* phenyl imide fragments, dehydrogenation of aniline leads to the release of two H atoms, and if these lead to hydroxylation of the surface bridging oxygen atoms (Fig. 2), some charge transfer is to be expected. We note, however, that our O 1s spectra (recorded at a much lower kinetic energy, and thus under much more surface-specific conditions than the conventional laboratory-source XPS used in the earlier study) show no evidence of the appearance of a low kinetic energy shoulder with a chemical shift of ~1.3 eV expected for hydroxyl species on this surface (e.g. [12]). As the STM and LEED results of Li and Diebold show a c(2x2) molecular overlayer, consistent with a coverage of the molecular species of 0.5 ML, achieving this coverage of phenyl imide from aniline would release 1 ML of atomic hydrogen. The absence of any significant OH feature in the O 1s spectrum indicates that the hydroxyl coverage must be very significantly less than 1 ML, so only a small fraction of the released H atoms can be bonded to the surface oxygen atoms and we can only surmise that most (or all) of the H atoms are desorbed as H_2 or are absorbed below the surface; on the basis of previous studies of hydrogen absorption and desorption [13, 14], the latter option seems the more probable.

Fig. 4 shows the C K-edge NEXAFS spectra (measured in the Auger electron detection

mode) obtained from these same surface preparation treatments. The spectra are rather noisy (particularly from azobenzene, for which a lower coverage was achieved) and there are significant variations in the background shape, but it is clear that the main features of the spectra recorded from surfaces exposed to azobenzene or to aniline occur at the same energies with similar relative intensities. In all of these spectra the main features are the three peaks at photon energies of ~285 eV, ~286 eV and ~288.5 eV, although the third of these peaks occurs in an energy range of varying background and is more or less clearly visible in the various spectra. The appearance of two peaks at energies of 284.9-285.5 eV and 288.6-289.4 eV, the exact energies being dependent on whether the molecule is in the gas phase or in monolayer or multilayer adsorption, is seen in NEXAFS spectra from benzene; both peaks are attributed to transitions from the C 1s state to final states of π-symmetry, and are thus characteristic of an intact aromatic ring [15]. The splitting of the lower-energy peak into two components separated by ~ 1 eV is also seen in molecular aniline [15, 16] and is attributed to the inequivalence of the C atoms within the aromatic ring that are, or are not, bonded to N. The appearance of these three peaks is thus entirely consistent with the surface molecular species arising from both reactants having both the aromatic ring and the attached N atom, as in phenyl imide.

NEXAFS data also provides information on molecular orientation. In particular, transitions from the 1s state to final states of π-symmetry in a planar molecule are only possible when there is a component of the electric vector, **A**, of the incident radiation perpendicular to the molecular plane. Indeed, the intensity of the relevant peak in the NEXAFS spectrum is proportional to $\cos^2(\alpha)$, where α is the angle between **A** and the normal to the molecular plane. For example if the molecular plane were to be perpendicular to the surface and aligned in the [001] azimuth, then at normal incidence with linearly-polarised radiation (i.e. at a grazing incidence angle, θ_p, of 90°, which also corresponds to the angle between the surface normal and **A**), there should be no π-resonance visible with incidence in the [001] azimuth, but a π-resonance of maximum intensity with incidence in the $[1\bar{1}0]$ azimuth. Indeed, the absence of a π-resonance peak in the spectrum for incidence in the [001] azimuth should also be true if the molecular

plane is tilted but remains aligned in the [001] azimuth. The absence of any obvious dependence of the NEXAFS spectra in Fig. 4 on the incidence azimuth thus shows that the phenyl imide is not aligned in either of the principle azimuths; either it is aligned in an intermediate low-symmetry direction, or is randomly oriented (possible rotating about the N-surface bond(s)). The selection rule also shows that if the molecular plane is parallel to the surface, no π-resonance should be detected with normal incidence (**A**-vector in the surface plane) in either azimuthal direction. As this is clearly not the case, the molecule, is not lying flat on the surface. Finally, we note that if the molecular plane is perpendicular to the surface, no π-resonance should be detected with a grazing incidence angle of 0° (**A**-vector perpendicular to the surface). Of course, true zero grazing-angle incidence is not achievable in practice, but the spectra of Fig. 4 clearly show that at an angle of 10° the π-resonances are clearly visible, so this perpendicular orientation is unlikely. A more quantitative determination of the tilt angle requires quantification of the polarisation-angle dependence of the π-resonance intensities, which must be normalised to the underlying edge-jump in each spectrum. Unfortunately, as seen in Fig. 4, the background shape in the various spectra is such that, in at least several of the spectra (particular those measured at normal incidence) it is not really possible to identify a clear edge jump.

We therefore conclude simply that the C K-edge NEXAFS data show the adsorbed species contains an intact phenyl ring, with some inequivalence of C atoms in the ring that give rise to spectra essentially identical to those of molecular aniline, that the molecular plane is not aligned along either principle azimuth and is probably randomly oriented azimuthally, and that this plane is tilted relative to the surface normal, by an unspecified (but probably significant) amount.

As it is the presence and polarisation-orientation dependence of π-resonance features that are most informative in NEXAFS, N K-edge NEXAFS from phenyl imide is expected to be relatively featureless. By contrast, however, intact azobenzene contains a N=N double bond, so in this species a π-resonance should be observed, and indeed has been reported

previously in measurements from more complex azo-biphenyl derivatives [17]. An absence of this π-resonance in spectra recorded from the room-temperature deposition of azobenzene is therefore a clear spectral signature of the scission of the N=N bond. Fig. 5 shows these data, and indeed the spectra from the room-temperature deposition are dominated by broad peaks that are due not to true NEXAFS features, but to the fact that, at the energy window values set on the electron spectrometer (377 eV and 379 eV for the spectra recorded at 90° and 10° grazing incidence, respectively), photoemission peaks from the shallow core levels of TiO_2 pass through this window. In the data collected at 10° grazing incidence (in which this spurious broad peak is at a higher energy by 2 eV), a weak edge jump is visible at a photon energy of ~398.2 eV, but there is clearly no π-resonance peak here. In order to provide an internal consistency check on the significance of this absence, similar measurements were also made from a multilayer film of azobenzene deposited at a sample temperature of 140 K, and these results are also shown in Fig. 5. In this case an intense π-resonance peak is seen at the edge jump as expected, providing a clear contrast with the equivalent spectrum from the surface exposed at room temperature. Evidently room temperature exposure to near-saturation coverage does lead to N=N bond scission, as proposed by Li and Diebold. However, also shown in the bottom panel of Fig. 5 is a series of NEXAFS spectra obtained after the multilayer was heated briefly to increasing temperatures. In these spectra a residual π-resonance remains even after heating to significantly above room temperature. The reason for this difference from the spectra obtained following room temperature deposition is unclear, but it seems that the high-coverage adsorbed layer obtained from multilayer desorption is not completely dissociated in the same way as it is following room temperature deposition. Interestingly, Li and Diebold report evidence of adsorbed intact azobenzene at low coverage following room temperature exposure, so there appear to be some circumstances under which azobenzene does *not* dissociate on TiO_2(110).

3.2 PhD structure determination

Based on the results of Li and Diebold, reinforced by our own NEXAFS results summarised above, there is strong evidence that exposure of the TiO_2(110) surface to

either azobenzene or aniline leads to a common surface species which seems to be most likely to be phenyl imide, and we may anticipate that this must chemisorb through the N atom to the surface, most probably to one or two surface Ti atoms that are five-fold (under-) coordinated (Fig. 2). Analysis of N 1s PhD modulation spectra should therefore allow us to determine explicitly and quantitatively this adsorption geometry.

Fig. 6 shows a comparison of a subset of the PhD spectra, recorded in three different emission directions, after exposure to each of the reactant molecules. While there are clear differences in the fine structure, due in large part to experimental scatter (especially from the lower-coverage azobenzene exposure), the dominant long-period modulations, characterised particularly by the energies of the main minima, which arise from near-neighbour substrate scattering, are clearly closely similar in spectra recorded from the surface exposed to the two different reactants. This subjective judgement is supported by a calculated value of the *R*-factor between the two experimental data sets of 0.30; such a value in a experiment/theory comparison would indicate generally good agreement, and a higher value might be expected in an experiment/experiment comparison due to the role of noise in both sets of spectra. These data demonstrate that the local adsorption geometry of the N atom bonded to the surface, in the surface species produced by the two different reactants, is the same. Combined with the NEXAFS data indicating both reactants lead to a surface species with a similarly-oriented phenyl ring and also demonstrating the scission of the S=S bond in azobenzene, together with the XPS results and the earlier STM images [7], there can be little doubt that the two reactant molecules do lead to a common surface molecular species. Moreover, the PhD data show that if coadsorbed (or absorbed) atomic hydrogen is present following reaction with aniline, this must have little or no effect on the local adsorption geometry of the adsorbed phenyl imide species.

In order to extract quantitative structural information from PhD data it is necessary to perform multiple scattering simulations of the experimental data for different structural models, adjusting the models until the best agreement is achieved. In many cases, however, some initial indication of the structure can be obtained from visual inspection of

the PhD modulation spectra. In particular, it is generally found that if the emission direction corresponds to near-180° backscattering from a nearest-neighbour substrate atom, the PhD spectrum is dominated by a single long-period modulation associated with the short scattering path from this one neighbouring atom. Thus, if the emitter atom is atop its nearest-neighbour substrate atom, this condition is met for emission along the surface normal, and this simple dominance of a single period is lost if the polar emission angle is increased substantially. The spectra shown in Fig. 6, all recorded near normal emission, do show this kind of underlying long-period modulation, while spectra recorded at much larger emission angles lose this character, and indeed are in most cases too noisy to be useful in the full analysis. This preliminary inspection, therefore, suggests that the molecule may be bonding to the surface with the N in, or close to, a site atop a surface (5-fold coordinated) Ti atom.

In order to achieve a proper quantitative analysis of the PhD data, however, we have undertaken a search of possible structures with the aid of multiple scattering calculations using the computer codes developed by Fritzsche [18, 19, 20]. These are based on the expansion of the final state wave-function into a sum over all scattering pathways that the electron can take from the emitter atom to the detector outside the sample. The agreement between theory and experiment was quantified using an objective reliability factor (*R*-factor) [9, 10], similar to that defined by Pendry for quantitative LEED studies [21]. This approach also allows us to define a criterion for the precision of the analysis and the relatively acceptability of different possible structural solutions. Specifically, we define a variance in the minimum value of the *R*-factor, R_{min}, (obtained for the best-fit structure) that depends on the size of the data-set used in the analysis [9, 10]. We then regard all structures having values of $R < R_{min} + \mathrm{var}(R_{min})$ as falling within the limits of our precision.

The calculations explored two basic structures, namely N bonding to a single 5-fold coordinated Ti surface atom in a near-atop site, or N bonding to two such surface Ti atoms in or near a bridging site. Optimisation of the fit for each of these models involved adjusting the exact location of the N emitter both perpendicular and parallel to the

surface, and varying the relaxation of the near-surface Ti and O atoms, the orientation of the attached phenyl ring (but omitting the very weakly-scattering H atoms), and the vibrational amplitudes of the surface and bulk atoms.

Bearing in mind the N bonding in the intact azobenzene (N=N) and aniline (NH_2) molecules, it seems reasonable to anticipate that the N atom of phenyl imide may bond to the TiO_2 surface in a bridging site to create two Ti-N bonds, and indeed this configuration was depicted in the cartoon of the reaction by Li and Diebold [7], although these authors made no claim to have determined this geometry. However, our attempts to fit the PhD data using this model failed to find a satisfactory solution. Fig. 7 shows a comparison of the set of five experimental N 1s PhD modulation spectra selected for the full analysis (on the basis of the size of the modulations and therefore data reliability), with the multiple scattering simulations for the best-fit bridging geometry found. The corresponding Ti-N bondlength is found to be 2.14 Å, but the overall *R*-factor value of 0.48 is rather large, consistent with the visual appearance of a poor fit. The fit to the normal emission spectrum is particularly bad, but lesser differences in the experimental and theoretical spectra at a polar emission angle of 30° in the [001] azimuth are also significant. In particular, a characteristic of the PhD technique is that in, or close to, an emission geometry corresponding to 180° scattering from a nearest-neighbour substrate atom, the spectrum is dominated by a single long-period modulation corresponding to backscattering from this atom. If the N emitter occupies this bridging site, this effect should be seen at a polar angle of ~40° in [001]. While we have no measurement in this exact geometry, a polar emission angle of 30° is sufficiently close for this effect to be seen in the simulated spectrum, which is dominated by a single period leading to three broad peaks that are damped at higher energies. By contrast, the experimental spectrum shows only the first of these peaks and is characterised by weak finer structure at higher energies. The absence of this clear long-period modulation in the experimental spectrum recorded at 30° is thus further evidence that N is not in this bridge-bonded site.

By contrast, exploration of the optimised geometry associated with the N atom near an atop site led to much better agreement between simulations and experiment, but with fits

of closely comparable quality at two quite different Ti-N bondlengths. These results are shown in Fig. 8. The two alternative values of the Ti-N bondlength are 1.77±0.05 Å and 2.27±0.04 Å, with associated *R*-factor values of 0.36 and 0.31, respectively. Visual inspection of the comparison of the simulated PhD spectra with the experimental data shows that both solutions are greatly superior to that achieved for the bridging site (Fig. 7), and indeed that these two alternative atop geometries give comparably-good agreement overall, the simulated spectra for the shorter bondlength being slightly preferred at the higher emission angles, while those of the longer bondlength give slightly superior fits near normal emission. The bottom panel of Fig. 8 shows how the R-factor varies as a function of the Ti-N bondlength if the remainder of the structural parameters (notably the near-surface relaxations) are fixed at the values corresponding to each of two best-fit structures. Notice that, depending on the values of these secondary structural parameters, either bondlength can yield the lower *R*-factor, but if we compare the best set of all parameters for each solution, that with the longer bondlength gives the lowest value, as given above. Unfortunately, the variance calculated for this value of R_{min} is 0.06, so the *R*-factor value for the short bondlength solution of 0.36 is below R_{min} + var(R_{min}) =0.37 and must also be regarded as acceptable. This problem of multiple coincidences at different bondlengths is well-documented in PhD [22], and also in the closely related method of quantitative LEED [23]; the general solution to the problem is to enlarge the data-set which lowers and variance and generally also increases the difference in the *R*-factors of the alternative solutions. In the present case the weak modulations and thus relatively poor signal-to-noise ratio of the PhD spectra recorded at other emission angles meant that we were unable to adopt this solution.

4. Discussion and theoretical results

Based on this analysis of the PhD data alone we must conclude that the phenyl imide bonds through the N atom in an atop site, and not a bridging site, relative to the undercoordinated Ti atoms in the surface, but that we are unable to distinguish between solutions with two very different Ti-N bondlengths. So far, however, we have not applied any constraints to the possible solutions based on other information, but the application of

such constraints is often a necessary component of *all* methods of structure determination. In the present case, a key question is whether the two alternative Ti-N bondlengths, 1.77±0.05 Å and 2.27±0.04 Å, are equally reasonable. In fact, particularly as we may expect this Ti-N bond to have a bond order of ~2, the longer bondlength seems quite unphysical. For example, NH bonded to a Ti atom in $TiCl_2(NH)(OPPh_3)_2$ has a Ti-N bondlength as short as 1.63 Å [24], while NH_2 bonded to a Ti atom in $Ti(NH_2)(Me_5C_5)_2$ has a Ti-N bondlength of 1.95 Å [25], similar to that (1.92 Å) in $N(CH_3)_2$ bonded to Ti in azatitanatranes [26]. Longer Ti-N bondlengths in the range 2.02-2.11 Å are found in titanium complexes bearing η^2-pyrazolato ligands in which a pair of adjacent N atoms in a five-membered ($N_2C_3R_2$) ring bond to a single Ti atom [27], while even longer Ti-N bonds of 2.33-2.40 Å have been reported, these are found in complexes in which the N atom that is bonded to the Ti atom is also bonded to three other atoms [28]. Comparison with these bondlengths in molecular clusters does suggest, therefore, that if phenyl imide is bonded to a single undercoordinated Ti atom on the TiO_2(110) surface, the Ti-N bondlength may be expected to be very significantly less than 2.27 Å, and probably less than 2.00 Å. We therefore favour the solution in which the Ti-N bondlength is 1.77±0.05 Å.

It is interesting to compare these conclusions with the results of a recent density functional theory (DFT) investigation [29, 30] of the adsorption and dissociation of azobenzene on TiO_2(110). The lowest-energy structure for phenyl imide on the surface found in this investigation does correspond to an atop adsorption site with the N bonding to a 5-fold coordinated Ti surface atom, in agreement with the conclusions of our PhD investigation. However, the Ti-N bondlength found in the DFT study of 2.07 Å is approximately midway between the two possible solutions found in the PhD analysis, and therefore clearly not consistent with our results. Moreover, in the DFT structure the phenyl ring is found to be perpendicular to the surface and parallel to the $[0\bar{1}1]$ azimuth, quite inconsistent with the results of our C K-edge NEXAFS measurements that indicate a tilted species not aligned along either principle azimuth. It is important to note, however, that this DFT study leads to relative energies that indicate that the dissociation

of azobenzene into two phenyl imide species on TiO_2(110) involves a very significant energy cost and should therefore not occur spontaneously. This has led the authors to concluded that this process 'still requires further investigation'. One possibility is that the common surface intermediate formed by reaction of azobenzene or aniline on TiO_2(110) is not phenyl imide but some other species that still retains a phenyl ring and bonds to the surface through a N atom. New DFT calculations aimed at exploring this possibility are currently under way [31].

Acknowledgements

The authors acknowledge the partial support of the Engineering and Physical Sciences Research Council (UK) for this work, and the award of synchrotron radiation beamtime at the BESSY facility. The computing facilities were provided by the Centre for Scientific Computing of the University of Warwick with support from the Science Research Investment Fund.

Figure Captions

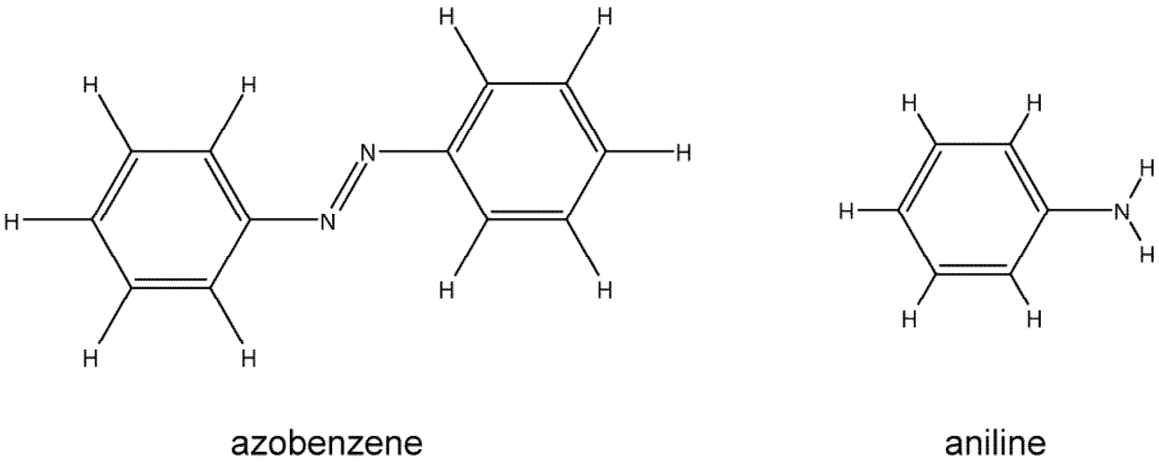

Fig. 1 the azobenzene and aniline molecules used in this study.

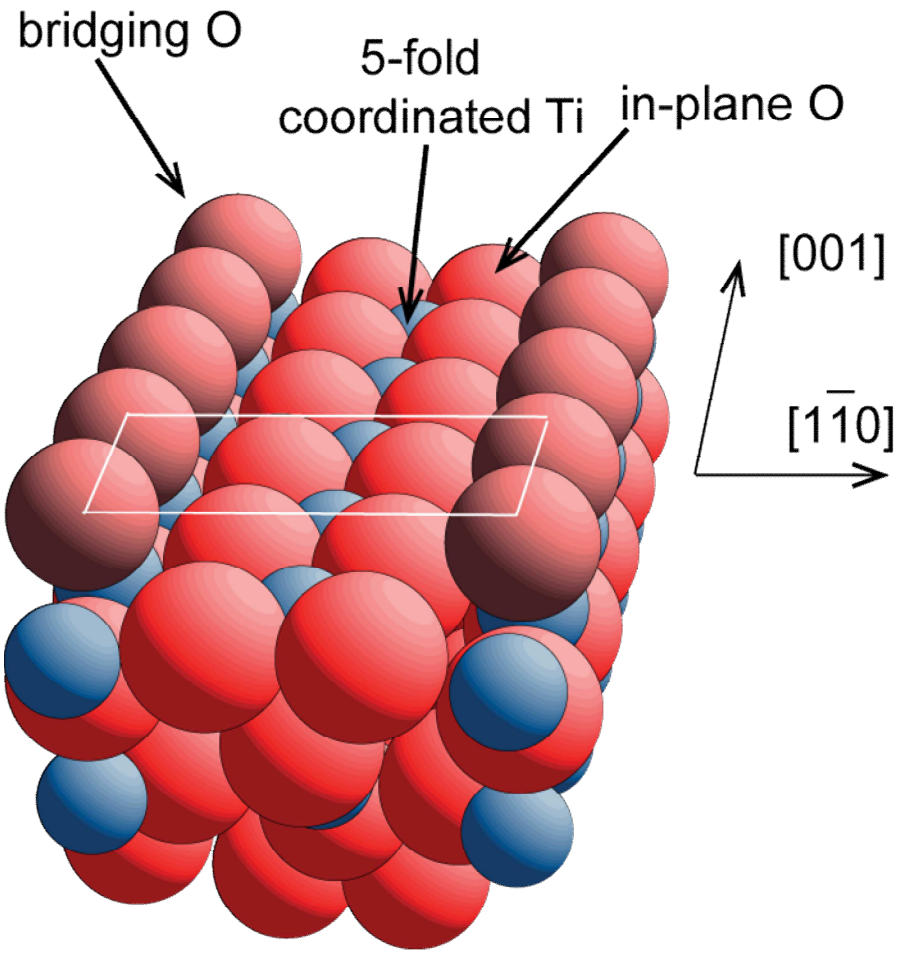

Fig. 2 Schematic diagram of the TiO_2(110) surface showing the different surface atoms and the azimuthal directions within the surface.

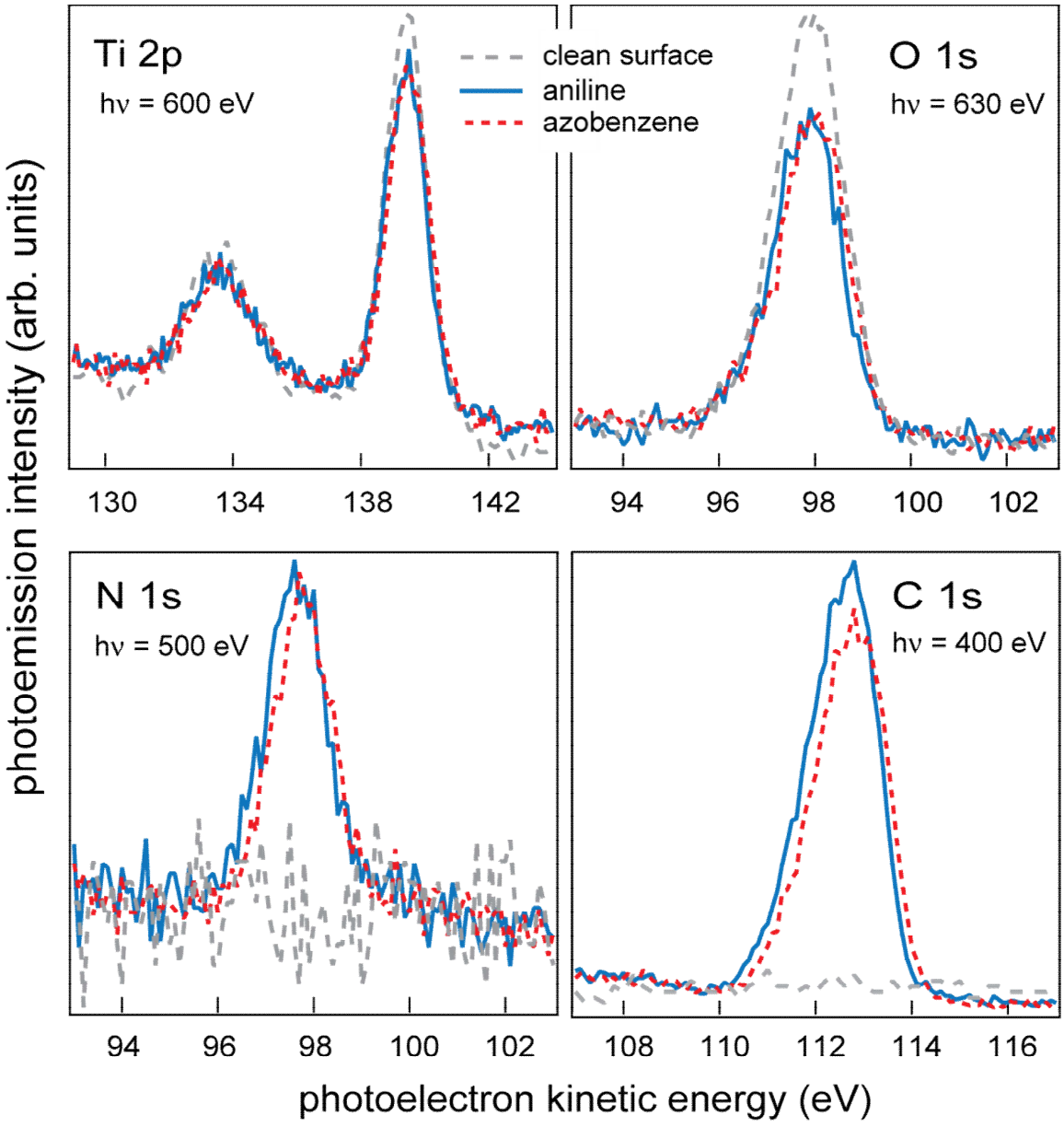

Fig. 3 SXP spectra from the clean TiO_2(110) surface and following exposure to aniline, and to azobenzene, at room temperature, recorded at normal emission.

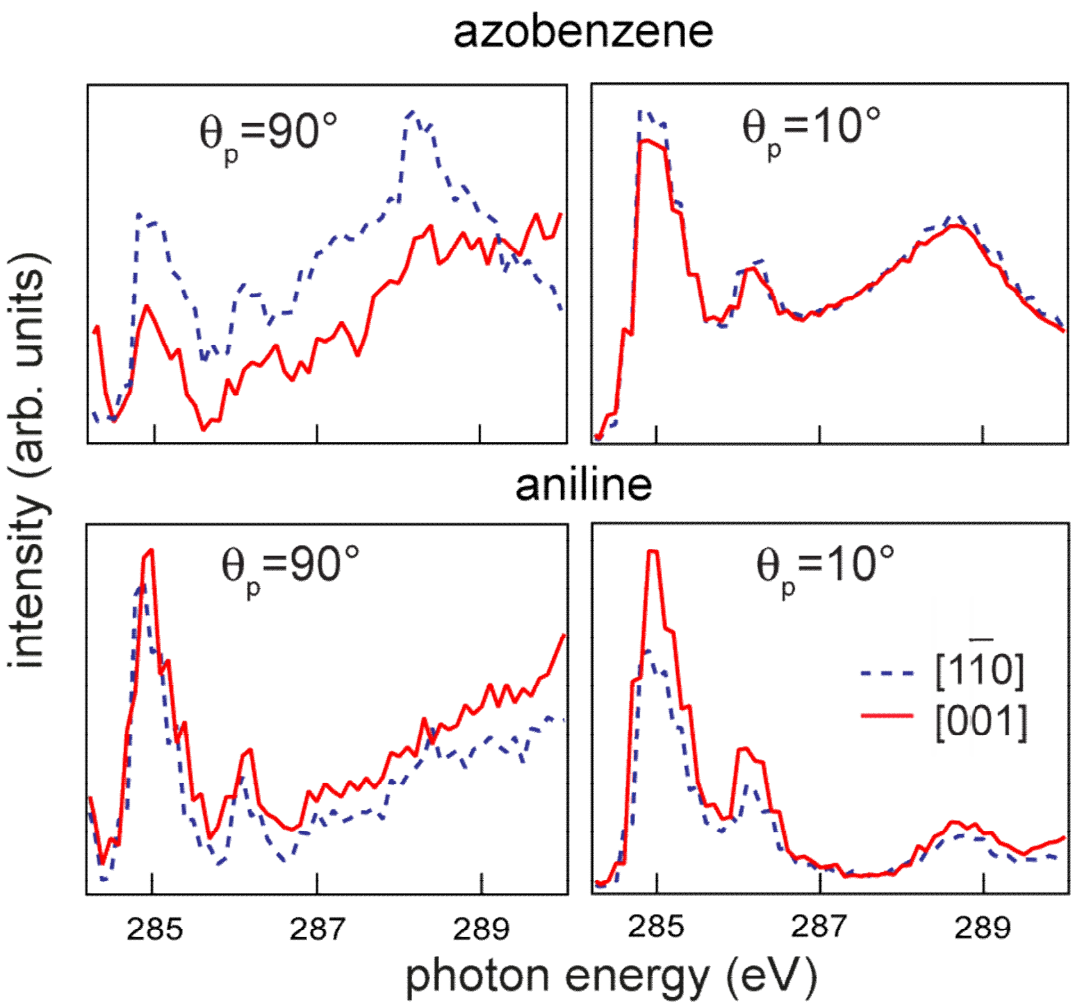

Fig. 4 C K-edge NEXAFS spectra from the TiO_2(110) surface following exposure to azobenzene, and to aniline, at room temperature. Spectra are shown for measurements in two different incidence azimuths (see Fig. 2), at each of two different incidence angle. θ_p is the *grazing* incidence angle (i.e. relative to the surface plane) and thus also the angle between the surface normal and the electric vector of the incident linearly-polarised radiation.

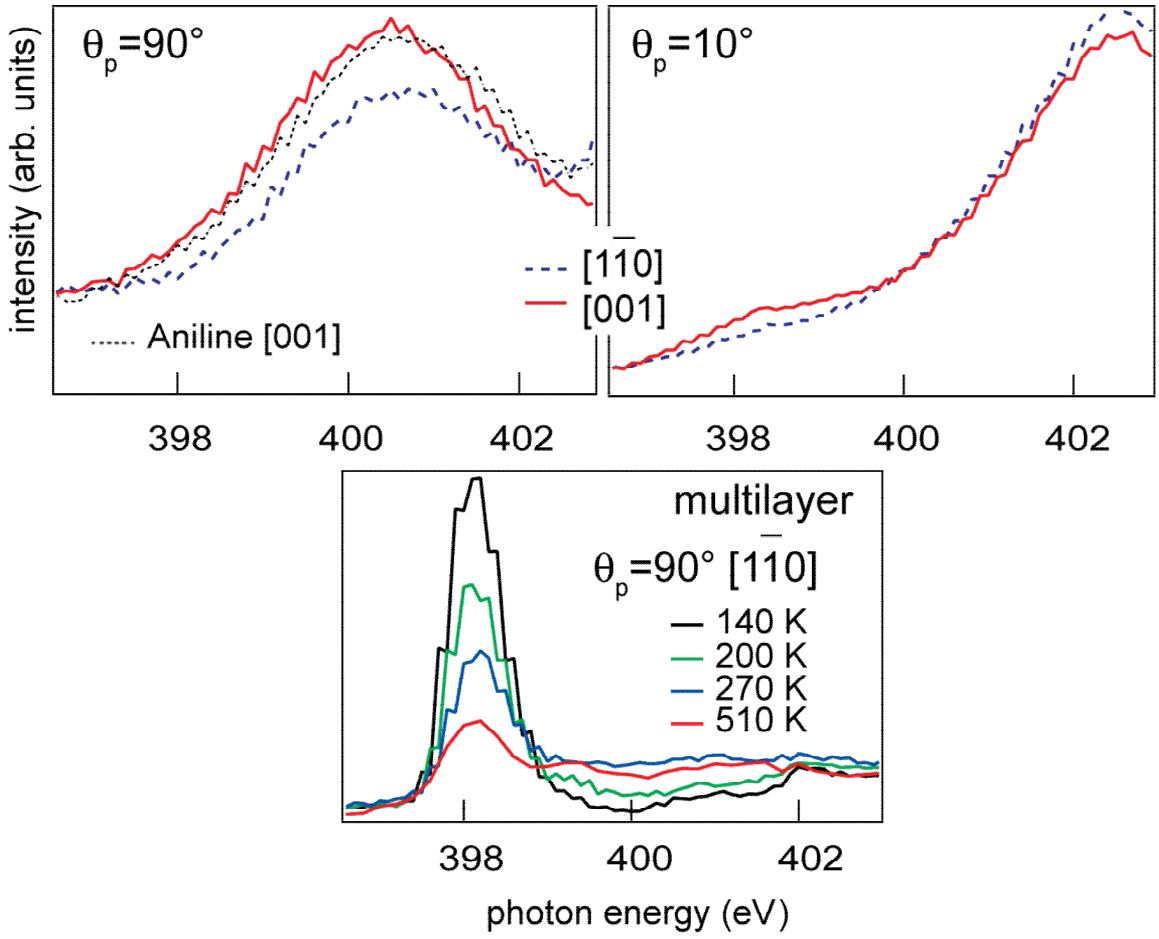

Fig. 5 N K-edge NEXAFS spectra from the TiO_2(110) surface following azobenzene exposure. The upper two panels show data obtained following exposure at room temperature, including one spectrum measured after aniline exposure. The panel below shows the spectrum recorded from an azobenzene multilayer deposited at 140 K, together spectra recorded after subsequent heating to increasing temperatures.

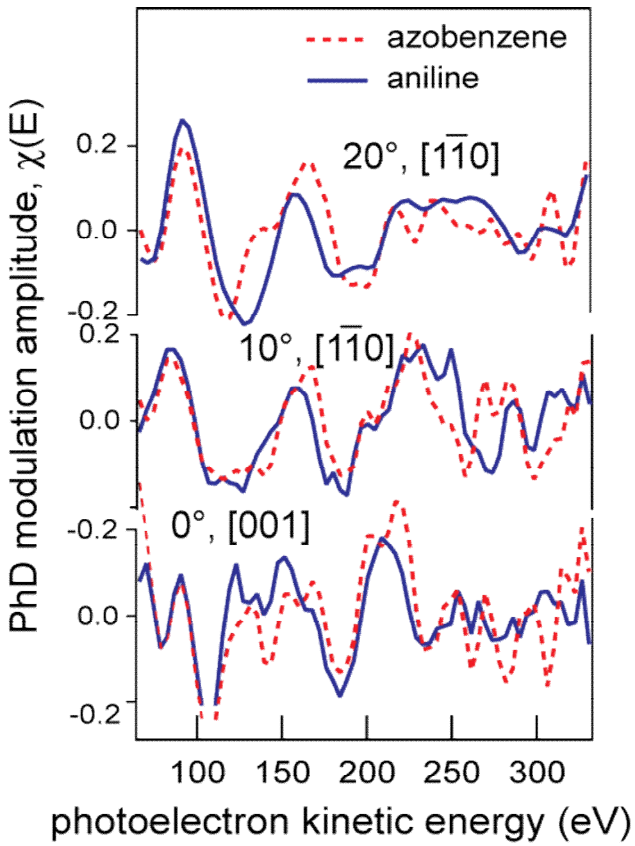

Fig. 6 Comparison of experimental N 1s PhD modulation spectra recorded in three different emission directions from the surface species formed by exposure of TiO_2(110) at room temperature to either azobenzene or aniline.

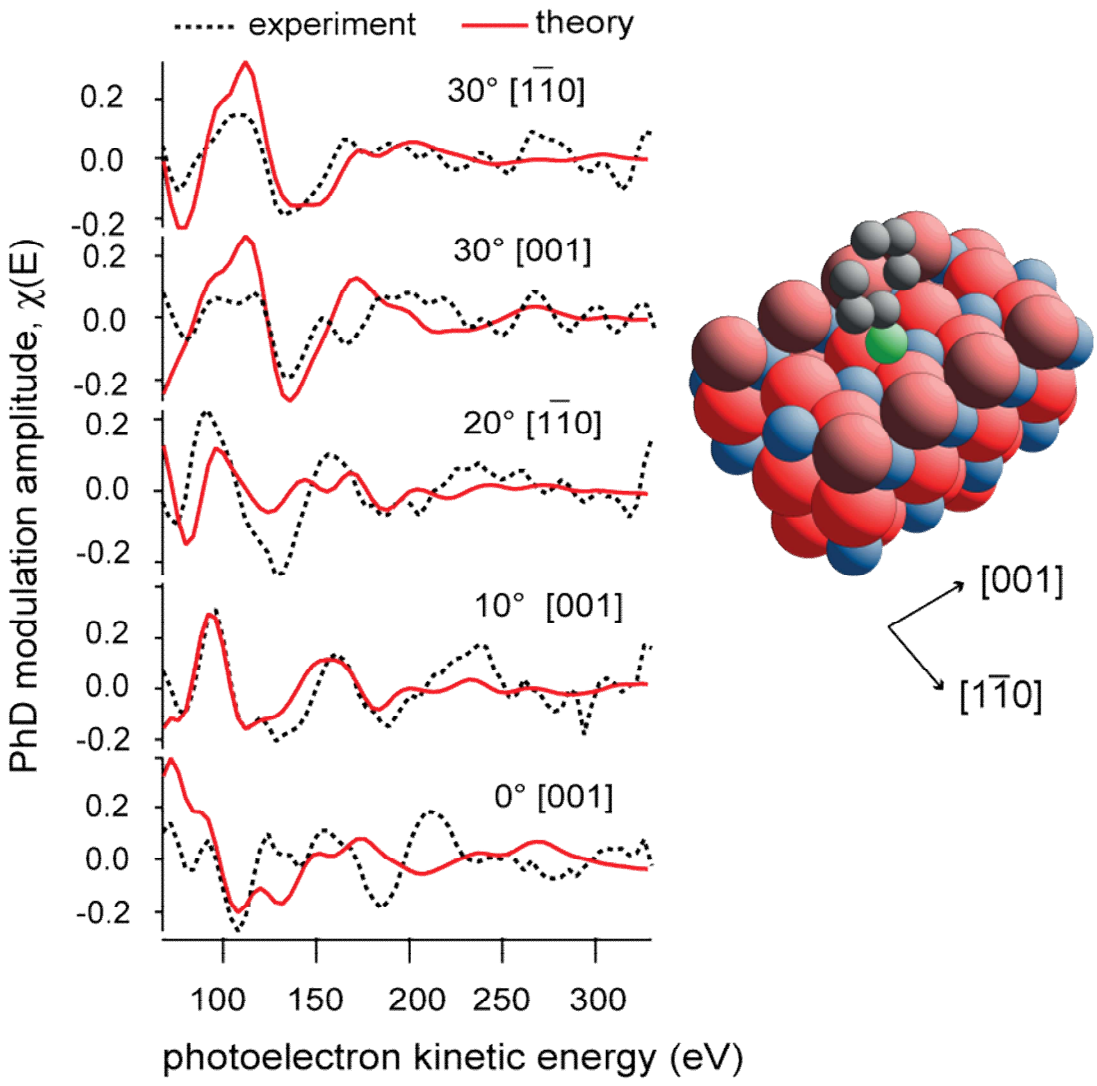

Fig. 7 Comparison of a set of five experimental N 1s PhD modulation spectra recorded from the azobenzene-dosed TiO_2(110) surface at room temperature, with the results of the best-fit multiple scattering simulations for adsorption with the N atom bridging an adjacent pair of surface undercoordinated Ti atoms (see schematic diagram on the right).

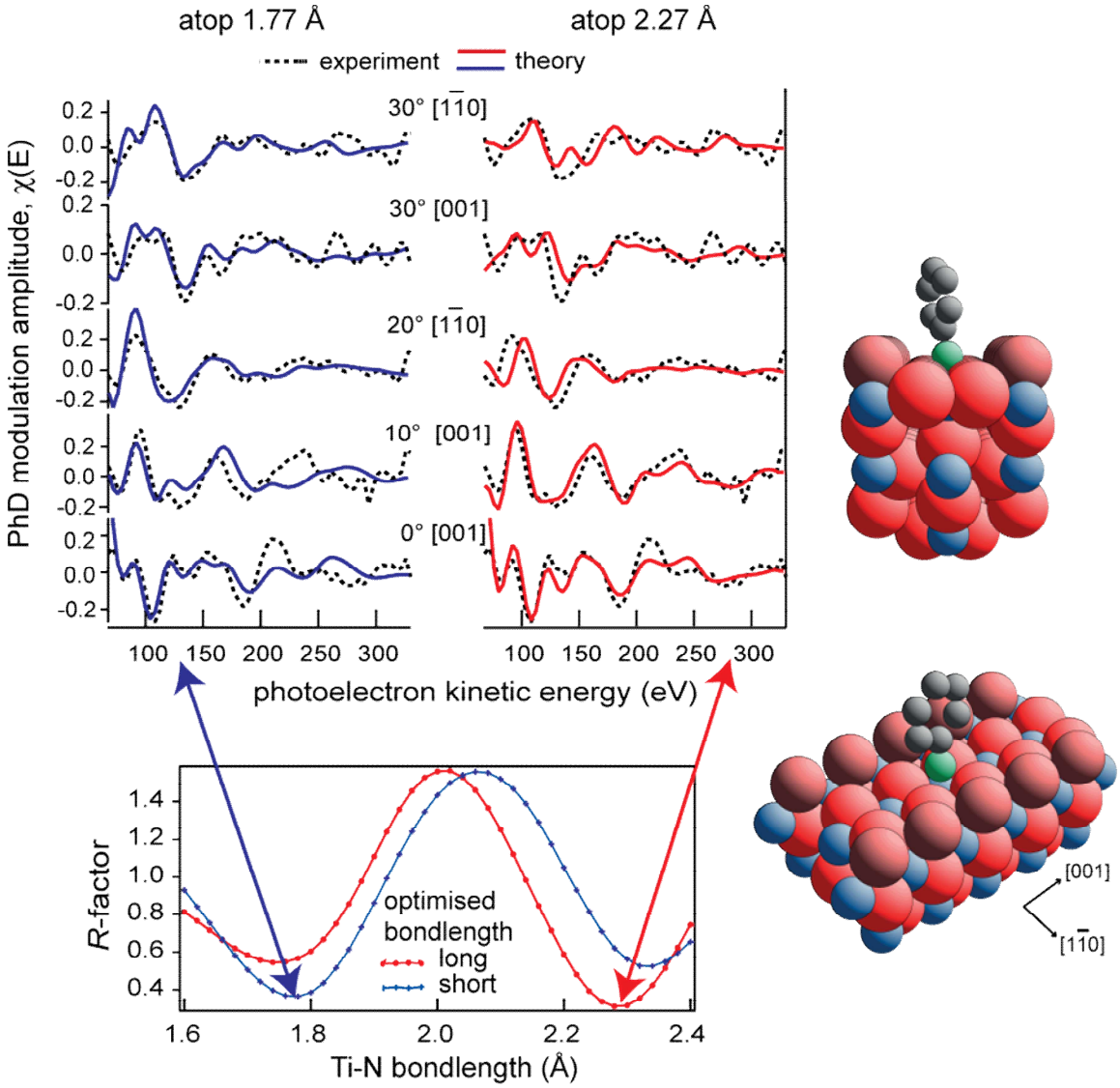

Fig. 8 Comparison of a set of five experimental N 1s PhD modulation spectra recorded from the azobenzene-dosed TiO_2(110) surface at room temperature, with the results of the best-fit multiple scattering simulations for adsorption with the N atom atop an undercoordinated surface Ti atom (see schematic diagram on the right). Results are shown for two different values of the Ti-N bondlength, while the bottom panel shows how the *R*-factor depends on this bondlength for the two alternative structural solutions.

References

1 U. Diebold, Surf. Sci. Rep. 48 (2003) 53.

2 M.A. Henderson, Surf. Sci. Rep. 46 (2002) 1.

3 C.L. Pang, R. Lindsay, and G. Thornton, Chem. Soc. Rev. 37 (2008) 2328.

4 M. Haruta, Catal. Today 36 (1997) 153.

5 A. Corma, P. Serna, Science 313 (2006) 332.

6 A. Grirrane, A. Corma, H. Garcia, Science 322 (2008) 1661.

7 S.-C. Li, U. Diebold, J. Am. Chem. Soc. 132 (2010) 64.

8 S.-C. Li, Y. Losovyj, V.K. Paliwal, U. Diebold, J. Phys. Chem. C 115 (2011) 10173.

9 D.P. Woodruff, A.M. Bradshaw, Rep. Prog. Phys. 57 (1994) 1029 .

10 D.P. Woodruff, Surf. Sci. Rep. 62 (2007) 1.

11 K.J.S. Sawhney, F. Senf, M. Scheer, F. Schäfers, J. Bahrdt, A. Gaupp, and W. Gudat, Nucl. Instrum. Methods A 390 (1997) 395.

12 W. Unterberger, T. J. Lerotholi, E. A. Kröger, M. J. Knight, D. A. Duncan, D. Kreikemeyer-Lorenzo, K. A. Hogan, D. C. Jackson, M. Sierka, R. Włodarczyk, J. Sauer, D. P. Woodruff, Phys. Rev. B, 84 (2011) 115461.

13 X.-L. Yin, M. Calatayud, H. Qiu, Y. Wang, A. Birkner, C. Minot, Ch. Wöll, ChemPhysChem 9 (2008) 253.

14 D.A.Panayotov, J.T. Yates, Jr., Chem. Phys. Lett. 436 (2007) 204.

15 J.L. Solomon, R.J. Madix, J. Stöhr, Surf. Sci. 255 (1991) 12.

16 S.X. Huang, D.A. Fischer, J.L. Gland, J. Phys. Chem. 100 (1996) 10233.

17 M. Elbing, A. Blaszczyk, C. von Hänisch, M. Mayor, V. Ferri, C. Grave, M.A. Rampi, G. Pace, P. Samori, A. Shaporenko, M. Zharnikov, Ad. Funct. Mater. 18 (2008) 2972.

18 V. Fritzsche, Surf. Sci., 265 (1992) 187.

19 V. Fritzsche, J. Phys.: Condens. Matter 2 (1990) 1413.

20 V. Fritzsche, Surf. Sci., 213 (1989) 648.

21 J.B. Pendry, J. Phys. C: Solid State Physics, 13 (1980) 937.

22 R. Dippel, K-U. Weiss, K-M. Schindler, D.P. Woodruff, P. Gardner, V. Fritzsche, A.M. Bradshaw, M.C. Asensio, Surf. Sci. 287/288 (1993) 465.

23 S. Andersson, J.B. Pendry, Solid State Commun. 16 (1975) 563.

24 P.J. McKarns, G.P.A. Yap, A.L. Rheingold, C.H. Winter, Inorg. Chem. 35 (1996) 5968.

25 E. Brady, J.R. Telford, G. Mitchell, Acta Cryst. C 51 (1995) 558.

26 F. Rioux, M.W. Schmidt, M.S. Gordon, Organometallics, 16 (1997) 158.

27 I.A. Guzei, A.G. Baboul, G.P.A. Yap, A.L. Rheingold, H.B. Schlegel, C.H. Winter, J. Am. Chem. Soc. 119 (1997) 3387.

28 Y. Sarazin, R.H. Howard, D.L. Hughes, S.M. Humphrey, M. Bochmann, Dalton Trans. (2006) 340

29 J.P. Prates Ramalho, F. Illas, Chem. Phys. Lett. 501 (2011) 379.

30 J.P. Prates Ramalho, F. Illas, Chem. Phys. Lett. 545 (2012) 60.

31 M.K. Bradley, J. Robinson, D.P. Woodruff, to be published.